Journal of Sound and Vibration (1998) **215**(1), 17–34
Article No. sv981640

A CONTINUOUS CRACKED BEAM VIBRATION THEORY

T. G. Chondros
University of Patras, 265 00 *Patras*, *Greece*

A. D. Dimarogonas
Washington University, *St Louis*, *MO* 63130-4899, *U.S.A.*

and

J. Yao
Siemens Medical Laboratories, *Concord*, *CA*, *U.S.A.*

(*Received* 5 *September* 1997, *and in final form* 17 *February* 1998)

A continuous cracked beam vibration theory is developed for the lateral vibration of cracked Euler–Bernoulli beams with single-edge or double-edge open cracks. The Hu–Washizu–Barr variational formulation was used to develop the differential equation and the boundary conditions of the cracked beam as a one-dimensional continuum. The displacement field about the crack was used to modify the stress and displacement field throughout the bar. The crack was modelled as a continuous flexibility using the displacement field in the vicinity of the crack, found with fracture mechanics methods. The results of two independent evaluations of the lowest natural frequency of lateral vibrations for beams with a single-edge crack are presented: the continuous cracked beam vibration theory developed here, and a lumped cracked beam vibration analysis. Experimental results from aluminum beams with fatigue cracks are very close to the values predicted. A steel beam with a double-edge crack was also investigated with the above mentioned methods, and results compared well with existing experimental data.

1. STATE OF THE ART

Vibration monitoring has great potential for machine condition monitoring. One form of damage that can lead to catastrophic failure if undetected is fatigue cracking of the structural elements [1–5]. Kirmsher [6], and Thomson [7] seem to be the earliest studies of vibrational characteristics of a beam with local discontinuities in the form of a small slot. A beam with different cross-sectional areas was used to replace the notched section of the beam.

A crack in an elastic structural element introduces considerable local flexibility due to the strain energy concentration in the vicinity of the crack tip under load. Long ago, this effect was recognized and the idea of an equivalent spring, a local compliance, was used to quantify in a macroscopic way the relation between the applied load and the strain concentration around the tip of the crack [8, 9]. This idea was mainly implemented in methods for determining an overall factor, describing the intensity of the stress concentration by measuring the local compliance of a cracked beam and relating it by energy arguments to the strain energy concentration and furthermore to the stress intensity factor. This became a standard method for experimental determination of the stress

0022–460X/98/310017 + 18 $30.00/0

intensity factor and a wealth of results, both analytical and experimental, were tabulated for a number of cases, different in loading and geometry, [10].

Liebowitz *et al*. [11], Liebowitz and Claus [12], and Okamura *et al*. [13] computed the local flexibility of a cracked bar in bending, which was used for column stability analysis. For stress analysis purposes, Rice and Levy [14] computed the local flexibility corresponding to tension and bending, including their coupling terms. Dimarogonas [15] introduced the local flexibility model of a crack for vibration analysis of cracked beams. Dimarogonas [16], Chondros [17], Chondros and Dimarogonas [18, 19], Dimarogonas and Massouros [20], combined this spring hinge model with the fracture mechanics results, and developed a frequency spectral method to identify cracks in various structures. This method correlated the crack depth to the change in natural frequencies of the first three harmonics of the structure for known crack position. Adams *et al*. [21], and Cawley and Adams [22] have developed an experimental technique to estimate the location and depth of the crack from changes in the natural frequencies.

Dimarogonas and Paipetis [23], and Anifantis and Dimarogonas [24] introduced a 5×5 local crack flexibility matrix neglecting torsion. Further, Dimarogonas and Paipetis [23] observed that this matrix was not purely diagonal but had off-diagonal terms which indicated the coupling between the longitudinal and lateral vibration.

Gudmundson [25], discussed a dynamic model for beams with transverse cracks. He showed that a cracked structural member could be represented by a consistent, static flexibility matrix. The results were compared to experimentally obtained eigenfrequencies. In the experiments, the cracks were modelled by saw cuts. The theoretical results for all crack lengths were in agreement with the experimental data. The dynamic stress intensity factor for a longitudinal vibration of the centrally cracked bar was determined as well. The results also compared very well with dynamic finite element calculations.

A full 6×6 matrix for an arbitrary loading of a cracked beam section finally was introduced by Papadopoulos and Dimarogonas [26], who computed this matrix analytically using fracture mechanics method. Finite element techniques were used for the same purpose by Haisty and Springer [27], Chondros and Dimarogonas [28].

Barr [29] and Christides and Barr [30] developed a cracked Euler–Bernoulli beam theory by deriving the differential equation and associated boundary conditions for a uniform Euler–Bernoulli beam containing one or more pairs of symmetric cracks. The reduction to one spatial dimension was achieved by using integration over the cross-section after certain stress, strain, displacement and momentum fields were chosen. In particular, the modification of the stress field induced by the crack was introduced through a local experimental function which assumed an exponential decay with the distance from the crack and included a parameter that had to be evaluated by experiments. Some experiments on beams containing cuts to simulate cracks were briefly described. The change in the first natural frequency with crack depth matched closely by the theoretical predictions. To validate the theoretical results, Shen and Pierre [31, 32] used a two-dimensional finite element approach to determine the parameter that controls the stress concentration profile near the crack tip in the theoretical formulation without requiring the use of experimental results. They observed an agreement between the theoretical and finite element results.

The Christides and Barr beam theory is an important step in the right direction for the development of a rigorous cracked beam vibration theory. However, the assumption of the exponential term of the stress field about the crack is a limitation that can be easily lifted. Christides and Barr determined the exponent of the stress field experimentally thus limiting the applicability of the method, although the stress exponent has been reported not to change very much. Fracture mechanics allows the development of a consistent cracked beam vibration theory without assumptions for the stress field.

Thus, such a consistent continuous cracked beam vibration theory is developed here. A numerical solution is developed for the prediction of changes in flexural vibration of a simply supported beam with a single open-edge or a double-edge open surface crack. Fracture mechanics methods were used to model the crack as a continuous flexibility in the vicinity of the crack region investigating the displacement field. Although many experimental results exist, there is extensive confusion in the literature in distinguishing between a notch and a crack [33]. Saw cuts are used to model cracks. But, no matter how thin a cut is it will not behave as a crack. A thin cut results in a local flexibility substantially less than the local flexibility associated with a fatigue crack. To validate the theory developed, experiments on aluminum beams with fatigue cracks were performed. In addition, experimental data on steel beams [30] with double-edge surface cracks were used as well to evaluate the analysis presented here. The theoretical and experimental results were also compared with analytical results from the Christides and Barr theory.

2. CRACKED EULER–BERNOULLI BEAM—THE EQUATION OF MOTION

A Euler–Bernoulli beam with an open-edge single transverse surface crack is shown in Figure 1. Let the displacement components be denoted by u_i, the strain components by γ_{ij} and the stress components by σ_{ij} with $i, j = 1, 2, 3$ referring to Cartesian axes x, y, z (Nomenclature are defined in the Appendix). Let p_i be the momentum such that $T_m = 1/2\ \rho\delta_{ij}p_ip_j$ will be the kinetic energy density (δ_{ij} is the Kronecker's delta). For arbitrary independent variations δu_i, $\delta\gamma_{ij}$, $\delta\sigma_{ij}$, and δp_i, the extended Hu–Washizu variational principle, [29, 34, 35] was introduced in the form:

$$\int_V \{[\sigma_{ij,j} + F_i - \rho\dot{p}_i)\delta u_i + [\sigma_{ij} - W_{,\gamma_{ij}}]\delta\gamma_{ij} + [\gamma_{ij} - (1 - \tfrac{1}{2}\delta_{ij})(u_{i,j} + u_{j,i})]\delta\sigma_{ij}$$

$$+ [\rho\dot{u}_i - T_{m,p_i})\delta p_i\}\,\mathrm{d}V + \int_{S_g} [\bar{g}_i - g_i]\delta u_i\,\mathrm{d}S + \int_{S_u} [u_i - \bar{u}_i]\delta g_i\,\mathrm{d}S = 0, \qquad (1)$$

where, $W(\gamma_{ij})$ is the strain energy density function, ρ is the density of the material. F_i, g_i and u_i are, respectively, the body forces, the surface traction and the surface displacements. Moreover, V is the total volume of the solid and S_g and S_u are its external surfaces. The overbar denotes the prescribed values of the surface traction and the surface displacement. The prescribed surface tractions g_i are applied over the surface S_g and the prescribed displacements u_i over S_u. Together S_g and S_u make up the total surface of the solid. The

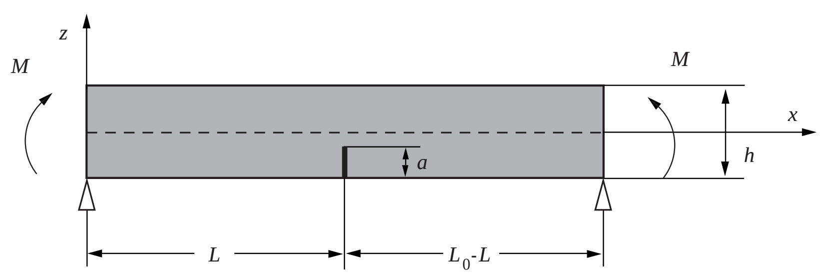

Figure 1. Geometry of a simply supported beam with an edge crack.

differentiation with respect to time ($\partial/\partial t$) is indicated by a dot. Commas in the subscripts indicate differentiation with respect to Cartesian axes.

To derive the governing equation and applicable boundary conditions for the transverse vibration of a cracked beam through the variational theorem, equation (1), the x-axis is taken along the centre line of the beam and the yz plane is the plane of the cross-section.

For an Euler–Bernoulli beam, in the absence of a crack, the displacement field is assumed in the form $u_1 = -zw'$, $u_2 = 0$, $u_3 = w(x, t)$. The strain field is assumed in the form $\gamma_{xx} = -zS(x, t)$, $\gamma_{yy} = \gamma_{zz} = -v\gamma_{zz}$, $\gamma_{xy} = \gamma_{xz} = \gamma_{yz} = 0$, where v is the Poisson ratio. The assumptions for γ_{yy} and γ_{zz} allow anticlastic curvature to develop freely. The stress field is assumed in such a way that the direct stress along the beam axis is of the form $\sigma_{xx} = -zT(x, t)$ while the only other non-zero stress is σ_{xz} due to lateral loading of the beam. The longitudinal or rotatory inertia and the shear deformation (p_x term) [30], are neglected as well as the transverse inertia (p_y term) associated with the anticlastic deformation. Thus, the momentum or velocity field is assumed to have the form $p_x = p_y = 0$, and $p_z = P(x, t)$.

The change in stress, strain and displacement distributions due to the crack will be expressed by a crack disturbance function for the axial displacement $f(x, z)$ introduced here.

For a uniform beam in the absence of body forces, the introduction of the displacement disturbance function $f(x, z)$ will modify equations (3) of reference [30] to yield:

$$u = -z\{[1 + f(x, z)]w(x, t)\}', \qquad \upsilon = 0, \qquad w = [1 + f(x, z)]w(x, t),$$

$$p_x = 0, \qquad p_y = 0, \qquad p_z = P(x, t),$$

$$\gamma_{xx} = -zS(x, t), \qquad \gamma_{yy} = \gamma_{zz} = -v\gamma_{xx}, \qquad \gamma_{xy} = \gamma_{yz} = \gamma_{xz} = 0,$$

$$\sigma_{xx} = -zT(x, t), \qquad \sigma_{xz} = \sigma_{xz}(x, z, t), \qquad \sigma_{xy} = \sigma_{zz} = \sigma_{xy} = \sigma_{yz} = 0,$$

$$F_x = F_y = F_z = 0, \tag{2}$$

where $u_1 = u$, $u_2 = \upsilon$, and $u_3 = w$ in the x, y, z directions, respectively.

Following the method introduced in reference [30] the term σ_{xz} is introduced for the lateral loading of the beam, and furthermore it will be noted $f(x, z) = f$. Equations (2) can now be substituted in the general variational theorem, equation (1) and independent variations of the unknowns w, P, S and T are considered. The variations will be considered one by one as follows.

For an arbitrary and independent variation δT, the strain–displacement term of equation (1) becomes:

$$\int_V \left[\gamma_{xx} - \frac{\partial u}{\partial x}\right]\delta\sigma_{xx}\,\mathrm{d}V = \int_x \left\{\int_A (-zS + z[(1+f)w]'') - z\delta T\,\mathrm{d}A\right\}\mathrm{d}x. \tag{3}$$

Defining the various integrals over the cross section A as

$$I = \int_A z^2\,\mathrm{d}A, \qquad I_2 = \int_A z\,\mathrm{d}A, \qquad I_4 = \int_A z^2 f''\,\mathrm{d}A,$$

$$I_5 = \int_A z^2 f'\,\mathrm{d}A, \qquad I_6 = \int_A z^2\;\mathrm{z}2\;(1+f)f\,\mathrm{d}A,$$

the right part of equation (3) becomes:

$$\int_x \{(I - 2I_2)S - (I_4 w + 2I_5 w' + I_6 w'')\}\delta T \, \mathrm{d}x. \tag{4}$$

The stress strain term in equation (1) is

$$\int_V \left\{\left[\sigma_{xx} - \frac{\partial W}{\partial \gamma_{xx}}\right]\delta\gamma_{xx} - \frac{\partial W}{\partial \gamma_{yy}}\,\delta\gamma_{yy} - \frac{\partial W}{\partial \gamma_{zz}}\,\delta\gamma_{zz}\right\}\delta S \, \mathrm{d}V, \tag{5}$$

where, $W = 1/2\lambda \mathrm{e}^2 + G(\gamma_{xx}^2 + \gamma_{yy}^2 + \gamma_{zz}^2) + 1/2G(\gamma_{xy}^2 + \gamma_{yz}^2 + \gamma_{xz}^2)$ the strain energy density, E is the Young modulus, $e = \gamma_{xx} + \gamma_{yy} + \gamma_{zz}$ is the dilatation, $G = E/[2(1 + v)]$ is the shear modulus, and $\lambda = vE/[(1 + v)(1–2v)]$ is the Lamé constant. Substituting the various quantities from equations (2) the stress–strain term (5) simplifies to:

$$\int_x \{(T - ES)(I - 2I_2))\, \delta S \, \mathrm{d}x. \tag{6}$$

The velocity momentum term is written using assumptions (2) as:

$$\int_x (\rho I_7 \dot{w} - \rho PA)\delta P \, \mathrm{d}x \tag{7}$$

where $I_7 = \int_A [1 + f(x, z)] \, \mathrm{d}A$.

The first term of equation (1) is the dynamic equilibrium term, which leads to the equation of motion. Using the assumptions of equations (2), this term becomes:

$$\int_V \left[\left(\frac{\partial \sigma_{xx}}{\partial x} + \frac{\partial \sigma_{xz}}{\partial z}\right)\delta u + \left(\frac{\partial \sigma_{xz}}{\partial x} - \rho \dot{P}_z\right)(1 + f)\delta w\right]\mathrm{d}V$$

$$= \int_A \int_x \left\{\left[(-zT)' + \frac{\partial \sigma_{xz}}{\partial z}\right]\left[-z\delta\left\{(1 + f)w\right\}'\right]\right.$$

$$\left. + \left(\frac{\partial \sigma_{xz}}{\partial x} - \rho \dot{P}\right)(1 + f)\delta w\right\} \mathrm{d}x \, \mathrm{d}A. \tag{8}$$

Since

$$\delta[(1 + f)w]' \equiv \frac{\partial}{\partial x}\,[(1 + f)\delta w], \tag{9}$$

the first term of equation (8) can be integrated by parts as

$$\int_A \int_x \left\{\left(z^2 T' - z\frac{\partial \sigma_{xz}}{\partial z}\right)\left(\frac{\partial}{\partial x}\right)[(1+f)\delta w]\right\} \mathrm{d}x\, \mathrm{d}A$$

$$= \int_A \left[z^2 T' - \left(z\frac{\partial \sigma_{xz}}{\partial z}\right)\right](1+f)\delta w\, \mathrm{d}A|_x$$

$$- \int_A \int_x \left[z^2 T'' - \frac{\partial}{\partial x}\left(z\frac{\partial \sigma_{xz}}{\partial z}\right)\right](1+f)\delta w\, \mathrm{d}x\, \mathrm{d}A. \tag{10}$$

The last term of equation (10) integrated by parts over z results in

$$\int_x \frac{\partial}{\partial x}\left\{\int_y \int_z z\frac{\partial \sigma_{xz}}{\partial z}\, \mathrm{d}z\, \mathrm{d}y\right\}(1+f)\delta w\, \mathrm{d}x$$

$$= \int_y \int_x \frac{\partial}{\partial x}(z\sigma_{xz})(1+f)\delta w\, \mathrm{d}x\, \mathrm{d}y|_z$$

$$- \int_A \int_x \frac{\partial \sigma_{xz}}{\partial x}(1+f)\delta w\, \mathrm{d}x\, \mathrm{d}A. \tag{11}$$

The boundary terms of equation (10) incorporated with the other boundary conditions of the variational equation (1) yield

$$\int_A \left\{z^2 T' - z\frac{\partial \sigma_{xz}}{\partial z}\right\}(1+f)\delta w\, \mathrm{d}A|_x + \int_y \int_x \frac{\partial}{\partial z}(z\sigma_{xz})(1+f)\delta w\, \mathrm{d}x\, \mathrm{d}y|_z. \tag{12}$$

The first and second term of the right part of equation (10) incorporated in equation (8) reduce the latter to the form

$$\int_x \int_A [(-z^2 T)'' - \rho \dot{P}](1+f)\delta w\, \mathrm{d}A\, \mathrm{d}k. \tag{13}$$

Performing the double differentiation indicated and integrating over the cross-section in equation (13), the dynamic equilibrium term of equation (1) can be rewritten as

$$\int_x \{I_2'' T + 2I_2' T' + (I_2 - I)T'' - \rho A\dot{P}\}(1+f)\delta w\, \mathrm{d}x. \tag{14}$$

It will be assumed that the lateral surfaces S_g of the beams are free of external traction, i.e., all prescribed traction on lateral surfaces are zero. The surface force is obtained from the stress components as $g_i = \sigma_{ij} n_j$ where n_j is the direction cosine of the external normal to the surfaces with the co-ordinate directions. If the beam is uniform, the normal to its lateral surfaces will be at right angles to its axis so that n_x is zero. Thus, using equations (2), the surface forces g_i become:

$$g_x = \sigma_{xx}n_x + \sigma_{xy}n_y + \sigma_{xz}n_z = \sigma_{xz}n_z,$$
$$g_y = \sigma_{yx}n_x + \sigma_{yy}n_y + \sigma_{yz}n_z = 0,$$
$$g_z = \sigma_{zx}n_x + \sigma_{zy}n_y + \sigma_{zz}n_z = 0. \tag{15}$$

On the other hand, over the ends of the beam $x = 0$ and $x = L_0$, there are $n_x = -1$ and $n_x = 1$, respectively (assuming plane ends normal to the beam axis). From equations (15) g_x is reduced to $\pm\sigma_{xx}$ and g_z to $\pm\sigma_{xz}$. The prescribed forces at the ends, integrated over the section, correspond to an applied force or moment.

The surface integral in the general variational equation (1) thus takes the form, over the lateral surface of the beam at the limits of z, z_1 and z_2, and $z_2 > z_1$:

$$\int_x \int_y \{[0 - \sigma_{xz}]_{z=z_2}\,\delta u + [0 + \sigma_{xz}\}]_{z=z_1}\,\delta u\}\,\mathrm{d}y\,\mathrm{d}x,$$

which can be written as:

$$\left[\int_x \int_y -\sigma_{xz}\delta u\,\mathrm{d}y\,\mathrm{d}x\right]_{z_1}^{z_2}.$$

Using the relation $\delta u = -z(1+f)\delta w'$ and integrating by parts over x, the latter surface integral becomes:

$$\left[\left(\int_y z\sigma_{xz}(1+f)\delta w\delta y\right)\bigg|_x - \int_y \int_x \frac{\delta}{\delta x}(z\sigma_{xz})(1+f)\delta w\,\mathrm{d}x\,\mathrm{d}y\right]_{z_1}^{z_2}. \tag{16}$$

The second term of this integral cancels the final term of equation (12). The second term of equation (12) can be integrated by parts over z, and results in a term which cancels the first term of equation (16). The remaining terms of equation (12) applied to the boundaries of x are:

$$\int_A \{z^2T' + \sigma_{xz}\}(1+f)\delta w\,\mathrm{d}A|_x. \tag{17}$$

Similarly, for the prescribed forces, the surface integral of equation (1) over the ends of the beam at $x = 0$ and $x = L_0$, take the form:

$$\left[\int_A \{(\bar{X} - \sigma_{xx})\delta u + (\bar{Z} - \sigma_{xz})(1+f)\delta w\}\,\mathrm{d}A\right]_{x=L_0}$$
$$+\left[\int_A \{(\bar{X} + \sigma_{xx})\delta u + (\bar{Z} + \sigma_{xz})(1+f)\delta w\}\,\mathrm{d}A\right]_{x=0}. \tag{18}$$

The variation δw in equation (17) is arbitrary and independent, which gives at the boundary

$$\{\sigma_{xz} = -z^2T'\}|_x. \tag{19}$$

From equations (18) and (19) and using equations (2) for the quantities δu, δw and σ_{xx}, integration over the section can be performed. The resulting boundary terms take the form,

$$\left[\left\{-\int_A z\bar{X}\,\mathrm{d}A + (I_2 - \mathrm{I})\mathrm{T}\right\}(1+f)\delta w'\right.$$

$$\left.+\left\{\int_A \bar{Z}\,\mathrm{d}A + (I - I_2)T' - I_2' T\right\}(1+f)\delta w\right]_{x=L_0}$$

$$-\left[\left\{-\int_A z\bar{X}\,\mathrm{d}A - (I_2 - I)T\right\}(1+f)\delta w'\right.$$

$$\left.+\left\{\int_A \bar{Z}\,\mathrm{d}A + (I - I_2)T' - I_2' T\right\}(1+f)\delta w\right]_{x=0}. \tag{20}$$

On the other hand, for the prescribed displacements, the surface integral of the variational equation (1) over the ends $x = 0$, and $x = L_0$ is:

$$\left[\int_A \{(u - \bar{u})\delta\sigma_{xx} + (1+f)(w - \bar{w})\delta\sigma_{xx}\}\,\mathrm{d}A\right]_{x=L_0}$$

$$-\left[\int_A \{(u - \bar{u})\delta\sigma_{xx} + (1+f)(w - \bar{w})\delta\sigma_{xx}\}\,\mathrm{d}A\right]_{x=0}. \tag{21}$$

After substituting for u, w and σ_{xx} from equations (2) and integrating over the section, the surface integral (21) becomes:

$$\left[\left\{(I - I_2)(1+f)w' + \int_A \bar{u}z\,\mathrm{d}A\right\}\delta T + \{(w - \bar{w})A\}\delta\sigma_{xz}\right]_{x=L_0}$$

$$-\left[\left\{(I - I_2)(1+f)w' + \int_A \bar{u}z\,\mathrm{d}A\right\}\delta T + \{(w - \bar{w})A\delta\sigma_{xz}\}\right]_{x=0}. \tag{22}$$

The entire variational statement for the vibration of cracked Euler–Bernoulli beams can now be assembled by using equation (1) and the variational terms (4), (6), (7) and (14) along with the boundary terms given in equations (20) and (22). The variations δw, δP, δS, δT and $\delta\sigma_{xz}$ are regarded as independent so that equation (1) implies, for arbitrary values of these variations, that each term multiplied by them in the volume integral must independently be zero, which will give the following relations directly: the strain–displacement term (4) for δT yields

$$S = Q_1(x)w'' + Q_2(x)w' + Q_3(x)w, \tag{23}$$

where $Q_1(x) = I_6/(I - 2I_2)$, $Q_2(x) = 2I_5/(I - 2I_2)$, $Q_3(x) = I_4/(I - 2I_2)$; from the stress–strain term (6),

$$T = ES; \tag{24}$$

from the velocity momentum term (7),

$$P = \frac{I_7}{A}\dot{w}; \tag{25}$$

and from the dynamic equilibrium term (14),

$$I_2''T + 2I_2'T' + (I_2 - I)T'' - \rho A\dot{P} = 0 \tag{26}$$

or

$$[(I - I_2)T''] + \rho A\dot{P} = 0. \tag{27}$$

Equation (27) is the equation of motion. Substituting for T and P can be made in terms of the displacement w by using equations (23)–(27). The resulting equation of motion is

$$E[(I - I_2)(Q_1 w'' + Q_2 w' + Q_3 w)]'' + \rho I_7 \dot{w} = 0. \tag{28}$$

Equation (28) is the differential equation expressing the consistent beam behaviour for generally distributed displacement field. The boundary conditions appropriate to the equation of motion (28) are obtained by equating the surface integral (20) to zero in case of prescribed external forces, and the equivalent surface integral (22) to zero in case of prescribed displacements.

Thus, for a simply supported beam the boundary conditions are

$$\bar{w} = 0, \quad \bar{X} = 0 \quad \text{at} \quad x = 0 \quad \text{and} \quad \bar{w} = 0, \quad \bar{X} = 0 \quad \text{at} \quad x = L_0.$$

If cracks are absent from the beam, the functions f, I_2, I_4, I_5, Q_2, Q_3 are zero, Q_1 is unity and function I_7 is replaced by area A. The equation of motion (28) will reduce to

$$EI\ \partial^4 w(x, t)/\partial x^4 + A\rho\ \partial^2 w(x, t)/\partial t^2 = 0. \tag{29}$$

3. THE CRACK DISTURBANCE FUNCTION

To develop the differential equation for the cracked beam from the general equation (28) a cracked beam of length L_0 with both ends ($x = 0$, $x = L_0$) being simply supported, as shown in Figure 1, is loaded with a bending moment M. The cross-sectional width and height are b and h, respectively. A crack is located at the bottom edge of the beam at $x = L$. The lateral displacement w_0 and the axial displacement u_0 at the ends of the uncracked beam are [36, 37]:

$$w_0 = (M/2EI)[L_0^2 + v(h^2/4)], \qquad u_0 = -hML_0/2EI.$$

Under general loading, the additional displacements w^*, u^* and θ^* due to the presence of the initial moment M and the crack will be computed by Castigliano's theorem. If U_T is the strain energy due to the crack, Castigliano's theorem demands that the additional rotation θ^* is

$$\theta^* = \partial U_T/\partial M, \tag{30}$$

due to the initial moment M and the crack. The strain energy has the form

$$U_T = \int_0^a \frac{\partial U_T}{\partial a}\,\mathrm{d}a = b\int_0^a J_S\,\mathrm{d}a, \tag{31}$$

where a is the crack depth and the strain energy density J_s has a general form

$$J_s = \frac{1}{E'}\left[\left(\sum_{i=1}^{6} K_{Ii}\right)^2 + \left(\sum_{i=1}^{6} K_{IIi}\right)^2 + m\left(\sum_{i=1}^{6} K_{IIIi}\right)^2\right],$$

where $E' = E/(1-v^2)$ for plane strain, $K_{Ii}, K_{IIi}, K_{IIIi}$ are the stress intensity factors corresponding to the three modes of fracture, which result for every individual loading mode i.

The stress intensity factor for a single-edge cracked beam specimen under pure bending M (Figure 1), is [10]

$$K_I = \sigma_0\sqrt{\pi a}\cdot F_I(\alpha) \quad \text{where } \sigma_0 = 6M/bh^2, \qquad \alpha = \frac{a}{h},$$

$$F_I(\alpha) = 1{\cdot}12 - 1{\cdot}40\alpha + 7{\cdot}33\alpha^2 - 13{\cdot}1\alpha^3 + 14{\cdot}0\alpha^4,$$

which has an accuracy of $\pm 0{\cdot}2\%$ for $a/h \leqslant 0{\cdot}6$. The strain energy density function J_s is

$$J_s = \frac{K_I^2}{E'} = \frac{1-v^2}{E}\,\sigma_0^2\pi a F_I^2(\alpha), \tag{32}$$

where K_I is the stress intensity. Thus, equation (30) yields the additional rotation θ^* as

$$\theta^* = 6\pi(1-v^2)Mh\Phi_I(\alpha)/EI, \tag{33}$$

where

$$\Phi_I(\alpha) = 0{\cdot}6272\alpha^2 - 1{\cdot}04533\alpha^3 + 4{\cdot}5948\alpha^4 - 9{\cdot}9736\alpha^5 + 20{\cdot}2948\alpha^6 - 33{\cdot}0351\alpha^7 + 47{\cdot}1063\alpha^8 - 40{\cdot}7556\alpha^9 + 19{\cdot}6\alpha^{10}.$$

On the other hand, assuming u_0 and u^* are the elongation of the lower surface of the beam due to the bending moment and the existence of the crack, respectively, the following geometric relations hold

$$\theta^*/\theta_0 = u^*|x-L|/L_0/u_0. \tag{34}$$

Since $\theta_0 = L_0M/EI$, equation (34) yields

$$\theta^* = 2u^*|x-L|/L_0/h. \tag{35}$$

From equations (2) it is $u^* = -zf'w_0$ and consequently, the crack disturbance function derivative will be:

$$f' = -6\pi(1-v^2)h^2\Phi_I(\alpha)(x-L)/zL_0(L_0^2 + vh^2/4), \tag{36}$$

which after integration over x yields the crack disturbance function

$$f = -6\pi(1-v^2)h^2\Phi_I(\alpha)(x-L)^2/zL_0(L_0^2 + vh^2/4). \tag{37}$$

For a cracked beam with a rectangular cross-section of height h and width b (Figure 1), the functions I, I_2, and I_7 defined in equations (3) and (7) are calculated as:

$$I = Ah^2/12, \qquad I_2 = \int_A z(x,z)\,\mathrm{d}A = 0, \qquad I_7 = \int_A [1 + f(x,z)]\,\mathrm{d}A. \tag{38}$$

The functions $Q_1(x)$, $Q_2(x)$ and $Q_3(x)$ defined in equation (23) now become:

$$Q_1(x) = I_7(x)/A, \qquad Q_2(x) = 2I_7'(x)/A, \qquad Q_3(x) = I_7''(x)/A. \tag{39}$$

The characteristic equation (27) of the cracked beam changes to

$$c_0^2[(I_7 w)^{iv}] + I_7 \ddot{w} = 0, \tag{40}$$

where $c_0^2 = EI/(\rho A)$ is a material constant.

From equation (40) it can be seen that the displacement disturbance factor $f(x, z)$ directly affects the displacement $w(x, t)$ through the function $I_7(x)$. The appropriate boundary conditions and initial conditions will be used to solve the last differential equation.

4. NATURAL FREQUENCIES OF A CRACKED BEAM

Consider a beam, as shown in Figure 1, with an open-edge crack at a distance L from the left end. The boundary conditions are:

$$w|_{x=0} = 0, \qquad \partial^2 w/\partial x^2|_{x=0} = 0, \qquad w|_{x=L_0} = 0, \qquad \partial^2 w/\partial x^2|_{x=L_0} = 0. \tag{41}$$

The differential equation for the natural modes can be written as:

$$[I_7(x)W(x)]^{iv} + \left(\frac{\omega_n^*}{c_0}\right)^2 [I_7(x)W(x)] = 0, \tag{42}$$

where ω_n^* are the natural frequencies of the cracked beam.

Solving equation (42) along with the associated boundary conditions (41), the solution is found as:

$$W(x) = \phi(x)[G_n \cos(\beta_n^* x) + H_n \cosh(\beta_n^* x) + A_n \sin(\beta_n^* x) + D_n \sinh(\beta_n^* x)], \tag{43}$$

where $\omega_n^* = c_0 \beta_n^{*2}$ are the natural frequencies of the cracked beams, G_n, H_n, A_n and D_n are constants, and $\phi(x) = 1/I_7(x)$ is the shape disturbance function associated with the crack disturbance function $f(x, z)$. Since $w = 0$ at $x = 0$, equation (43) yields $G_n = 0$, $H_n = 0$, and consequently

$$W(x) = \phi(x)[A_n \sin(\beta_n^* x) + D_n \sinh(\beta_n^* x)]. \tag{44}$$

The boundary conditions at $x = L_0$ give:

$$A_n \sin(\beta_n^* L_0)\phi(L_0) + D_n \sinh(\beta_n^* L_0)\phi(L_0) = 0$$

$$A_n[-\phi(L_0)\sin(\beta_n^* L_0)\beta_n^{*2} + 2\phi'(L_0)\cos(\beta_n^* L_0)\beta_n^* + \phi''(L_0)\sin(\beta_n^* L_0)]$$
$$+ D_n[\phi(L_0)\sinh(\beta_n^* L_0)\beta_n^{*2} + 2\phi'(L_0)\cosh(\beta_n^* L_0)\beta_n^* + \phi''(L_0)\sinh(\beta_n^* L_0)] = 0. \tag{45}$$

The system of equations (45) yields the characteristic equation

$$I_7'(L_0)/I_7(L_0)[\cos(\beta_n^* L_0) - \sin(\beta_n^* L_0)\coth(\beta_n^* L_0))] + \beta_n^* \sin(\beta_n^* L_0) = 0. \tag{46}$$

This implicit natural frequency equation (46) can be solved directly for an exact solution β_n^* through a numerical method. Results with the aforementioned procedure for the lateral vibration of a simply supported Euler–Bernoulli prismatic beam with an open crack located at mid-span are shown in Figure 2.

Results refer to an aluminum beam of length 0·235 m, cross-section width $b = 0{\cdot}006$ m, cross-section height $h = 0{\cdot}0254$ m, $E = 7{\cdot}2\text{E}10\ \text{N/m}^2$, material density $2800\ \text{kg/m}^3$ and Poisson ratio 0·35. The continuous beam theory results correlate well with the experimental data for crack depths up to 60%.

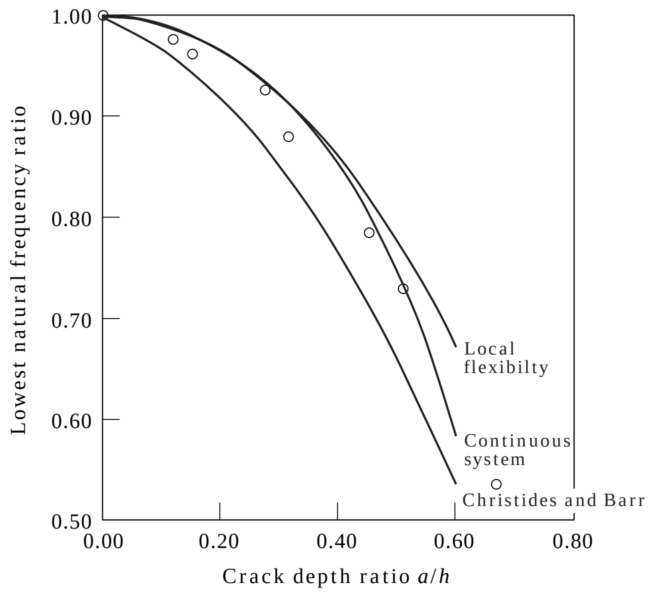

Figure 2. Lowest transverse natural frequency ratio ω_1^*/ω_1 for a simply supported beam with a surface crack at mid-span, versus the crack depth ratio $\alpha = a/h$. Analytical results: (a) continuous cracked beam model, equation (46); (b) lumped crack flexibility model, equation (48); (c) Christides and Barr's [30] theoretical results, equation (34). Experimental results: ○.

Also, in Figure 2, the current results of the continuous model for the first mode was compared with Christides and Barr's [30] theoretical results (equation (34)).

5. BEAM WITH LUMPED CRACK FLEXIBILITY

The above procedure distributes the added flexibility due to the crack over the length of the beam. For comparison, the natural frequencies of a cracked beam considering the crack as a local flexibility, was found. The local flexibility can be found from equation (33) as

$$c = 6\pi(1 - \nu^2)h\Phi_1(\alpha)/EI.$$

Assuming that the effect of the crack is apparent in its neighbourhood only, the beam can be treated as two uniform beams, connected by a torsional spring of local flexibility c at the crack location. The modes of harmonic vibration of the two segments of the beam, left and right of the crack, respectively, are

$$W_1(x) = A_1 \cos(\lambda x) + A_2 \cosh(\lambda x) + A_3 \sin(\lambda x) + A_4 \sinh(\lambda x),$$

$$W_2(x) = B_1 \cos(\lambda x) + B_2 \cosh(\lambda x) + B_3 \sin(\lambda x) + B_4 \sinh(\lambda x),$$

where the origin of x for both segments is at the left support, ω_{L_n} the natural frequencies of the cracked beam with lumped crack flexibility, $\lambda^2 = \omega_{L_n}/c_0$, and $c_0^2 = EI/(\rho A)$.

The coefficients A_i, B_i can be found by substituting this solution into the boundary condition equations. Assuming constant properties along the beam, the boundary conditions for the left and right parts of the beam are:

$$w_1|_{x=0} = 0, \quad w_2|_{x=L_0} = 0, \quad \partial^2 w_1/\partial x^2|_{x=0} = 0, \quad \partial^2 w_2/\partial x^2|_{x=L_0} = 0,$$

$$w_1|_{x=L} - w_2|_{x=L} = 0, \quad \partial^2 w_1/\partial x^2|_{x=L} - \partial^2 w_2/\partial x^2|_{x=L} = 0,$$

$$\partial^3 w_1/\partial x^3|_{x=L} - \partial^3 w_2/\partial x^3|_{x=L} = 0,$$

$$\partial w_2/\partial x|_{x=L} - \partial w_1/\partial x|_{x=L} = (EIc/L)L\partial^2 w_2/\partial x^2|_{x=L}, \tag{47}$$

where EIc/L is the non-dimensional cracked section flexibility. Defining a non-dimensional crack location measured from mid-point $\beta = (L - L_0/2)/(L/2)$ yields the natural frequency equation for the beam with lumped crack flexibility:

$$4 \sin \lambda L_0 \sinh \lambda L_0 + \lambda L_0(EIc/L)[\sinh \lambda L_0(\cos \lambda L_0 - \cos \beta\lambda L_0) + \sin \lambda L_0(\cosh\lambda L_0 - \cosh\beta\lambda L_0)] = 0 \tag{48}$$

Equation (48) is solved numerically to yield the natural frequencies ω_{L_n} as shown in Figure 2.

6. EXPERIMENTAL EVIDENCE

Prismatic beams made of aluminum of rectangular cross-section 7×23 mm and length 235 mm were prepared. Material properties are: Young's modulus of elasticity $E = 7{\cdot}2$ E10 N/m^2 and material density 2800 kg/m^3. At mid-span, a sharp notch was introduced perpendicular to the longitudinal axis and the longer dimension of the cross-section. Then, the beam was placed on a shaker table, with one end fixed and the other free and was vibrated at its lowest bending natural frequency for the purpose of initiating and propagating a fatigue crack. Different specimens were vibrated at different numbers of cycles so that different crack lengths would be obtained. To detect crack propagation, a transparent measuring scale was attached on the beam's side and a strobe light connected to the vibrating table power supply was used. When the desired crack depth was obtained, the beam was taken out of the vibrating table and the crack depth was measured on both sides of the beam. If the crack length was not symmetric on both sides of the beam, the specimen was rejected and the fatigue crack formation was repeated on a new specimen.

The crack was forced open to assure compliance with the open crack assumption of the analysis. Then, each beam was simply supported at the two ends by sharp knife-edged steel supports to assure free flexural motion. A small accelerometer of mass 1 g was fixed at mid-span on the surface of the beam opposite to the crack. To avoid bouncing the beam was lightly tapped with a miniature hammer and the resulting vibration signal was recorded and plotted. The vibration frequency was calculated by measuring the time elapsed for 50 cycles of vibration. Moreover, an FFT transform was performed on the stored signal for an independent measurement of the flexural natural frequencies. The lowest natural frequency of the short aluminum beams was around 1·6 kHz. The 100-kHz sampling rate two channel A/D converter used could give good accuracy for the fundamental frequency measurement.

The measurements were consistent up-to crack depths of slightly more than half the width height, $\alpha = a/h = 0{\cdot}6$. At larger depths, vibration coupling resulted in a crowded spectrum and a complex time signal so that the natural frequency could not be measured with confidence. Moreover, at depths smaller than $\alpha = 0{\cdot}1$ the difference from the natural frequency of the uncracked beam was not measurable. Therefore, experimental results will be limited here for α between 0·1 and 0·6. For each specimen the ratio of the undamaged to the cracked beam frequency was of importance thus eliminating the influence of minor differences in the frequencies of the uncracked specimen measured. Also, the experimental points are averages from tests but the spread of frequency measurements about the points was very small.

7. DOUBLE-EDGE SURFACE CRACK

The stress-intensity function K_I for a beam with a double-edge crack under the bending moment M is [10, 38]:

$$K_1 = \sigma_0\sqrt{\pi a}F_1(\alpha),$$

with

$$\sigma_0 = 6M/bh^2, \qquad \alpha = a/h$$

and

$$F_I(\alpha) = 1{\cdot}130 - 1{\cdot}374\alpha + 5{\cdot}749\alpha^2 - 4{\cdot}464\alpha^3 + 15{\cdot}25\alpha^6 - 9{\cdot}315\alpha^7 \quad \text{for } 0 \leqslant a \leqslant h/2.$$

In the above equations, a is the depth of the crack on each side of the beam, b is the thickness of the beam, and h is the height of the cross-section of the beam.

Equation (31) yields

$$U_T = 6(1 - v^2)M^2h\pi\Phi_1^2(\alpha)/E, \tag{49}$$

where

$$\Phi_I(\alpha) = 0{\cdot}63845a^2 - 1{\cdot}03508a^3 + 3{\cdot}72015a^4 - 5{\cdot}17738a^5 + 7{\cdot}55301a^6 - 7{\cdot}33244a^7 + 2{\cdot}49091a^8 - 2{\cdot}3391a^9 + 2{\cdot}55976a^{10} - 9{\cdot}7367a^{11} + 6{\cdot}93036a^{12} + 5{\cdot}42308a^{16},$$

and hence the additional rotation θ^* due to the crack will be:

$$\theta^* = 6\pi(1 - v^2)Mh\Phi_I(\alpha)/EI. \tag{50}$$

The displacement disturbance functions yield in a similar way as in equations (36) and (37) as:

$$f' = -12\pi(1 - v^2)h^2\Phi_I(\alpha)(L_0 - L)/L_0z(L_0^2 + vh^2/4)$$

and

$$f = h - 12\pi(1 - v^2)h^2\Phi_I(\alpha)(L_0 - L)^2/L_0^2(L_0^2 + vh^2/4).$$

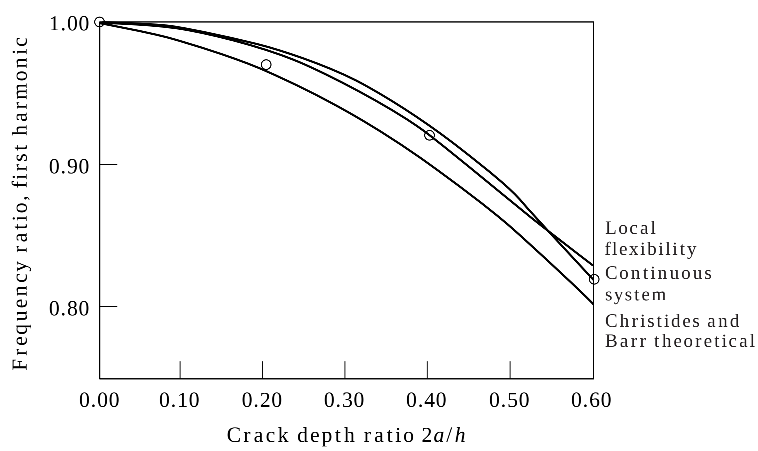

Figure 3. Lowest transverse natural frequency ratio ω_1^*/ω_1 for a simply supported beam with a double-edge surface crack at mid-span, versus the crack depth ratio $\alpha = 2a/h$. Analytical results: (a) lumped crack flexibility, equation (48); (b) continuous crack model, equation (46); (c) Christides and Barr's [30] theoretical results, equation (34). Experimental results [30]: ○.

The solution of the characteristic equation (46) for a beam with a double-edge crack is shown in Figure 3. Also, in Figure 3, the current result of the continuous model for the first mode was compared with Christides and Barr's [30] experimental results for a simply supported beam with a double-edge open crack at mid-span, symmetric with respect to the neutral axis and perpendicular to it. In the same figure, the lumped crack flexibility model equation (48), as well as the solution of the frequency shifting ratio equation (34) of reference [30] for the cracked beam are also shown. Beam data are $L = 0{\cdot}575$ m, $b = 0{\cdot}00952$ m, $h = 0{\cdot}03175$ m, $E = 2{\cdot}06\mathrm{E}11\,\mathrm{N/m^2}$, material density $\rho = 7800\,\mathrm{kg/m^3}$ and Poissson ratio $\nu = 0{\cdot}35$. The continuous cracked beam model provides results closer to the experimental data than Christides and Barr's theoretical results, and correlates well with the lumped crack flexibility model.

8. CONCLUSIONS

The continuous cracked beam vibration theory developed here, and the application to simply supported beams with a single- or a double-edge open surface crack led to a good approximation for the dynamic response to lateral excitation. This systematic cracked beam formulation is a generalization of Christides and Barr's cracked beam theory. The continuous cracked beam theory that has been developed by Christides and Barr [29, 30], a very important step towards a consistent crack beam theory, uses an experimentally defined crack disturbance function. The continuous cracked beam theory that has been developed by Wauer [38], a rigorous formalization of the local flexibility approach, uses the normalization of the local flexibility to develop a differential equation for the cracked beam. In the present formulation the transverse vibration model of the cracked beam is based on analytical expressions for the displacement field obtained with well-established methods in fracture mechanics and published experimental or analytical results for the stress intensity factor.

To validate the theory developed, experiments on aluminum beams with fatigue cracks were performed. Experimental results on aluminum beams with single-edge open cracks, and experimental data for steel beams with double-edge cracks obtained by Christides and Barr are very close to the continuous cracked beam formulation.

It is expected that the continuous cracked beam theory will be a useful alternative tool for vibration analysis of cracked structures, as it can be easily extended to other vibration modes, geometries and boundary conditions and to coupled lateral and torsional vibration problems. Changes in the fundamental frequency of cracked beams were investigated since it is of prime importance in engineering applications. Moreover, the continuous cracked beam differential equation formulation lends itself for further analysis, beyond the natural frequency calculation.

Finally, the continuous cracked beam formulation can be readily applied to the flexural vibration of beams with single- or double-edge surface cracks, and be extended to multiple cracks and other geometries and boundary conditions.

REFERENCES

1. J. M. Schmerling and J. C. Hammon 1966 *American Power Conference Chicago*, *IL*. Investigation of the Tennessee Valley Authority Gallation Unit No. 2 turbine rotor burst.
2. A. R. Jack and A. N. Patterson 1976 *First Mechanical Engineering Conference*. The influence of the environment on fatigue cracking in 500 MW LP rotor shafts.
3. H. Haas 1977 *Maschinenschaden* **50**, 195–204. Grossschäden durch Turbinen-oder Generatorleufer, entstanden im Bereich bis zur Schleuderdrehzahl.

4. J. GRECO, J. R. AGNEW, K. ERHARDT, J. E. BERTILSSON and Z. S. STYS 1978 *American Power Conference*, *Chicago*, *IL*. Cumberland steam plant-cracked IP rotor coupling.
5. J. BOHNSTEDT and L. LEOPOLD 1985 *Maschinenschaden* **58**, 81–88. Schaden und Reparaturen an Dampfturbinen.
6. P. G. KIRMSHER 1944 *Proceedings of the American Society of Testing and Materials* **44**, 897–904. The effect of discontinuities on the natural frequency of beams.
7. W. J. THOMSON 1943 *Journal of Applied Mechanics* **17**, 203–207. Vibration of slender bars with discontinuities in stiffness.
8. G. R. IRWIN 1957 *Journal of Applied Mechanics* **24**, 361–364. Analysis of stresses and strains near the end of a crack traversing a plate.
9. G. R. IRWIN 1958 in *Handbuch der Physik*, Volume **6**, 551–590. Heidelberg: Springer-Verlag, Fracture.
10. H. TADA 1973, 1985 *The Stress Analysis of Cracks Handbook*. Hellertown, Pennsylvania. Del Research Corporation.
11. H. LIEBOWITZ, H. VANDERVELDT and D. W. HARRIS 1967 *International Journal of Solids and Structures* **3**, 489–500. Carrying capacity of notched column.
12. H. LIEBOWITZ and W. D. CLAUS 1968 *Engineering Fracture Mechanics* **1**, 379–383. Failure of notched columns.
13. H. OKAMURA, H. W. LIU, C.-S. CHU and H. LIEBOWITZ 1969 *Engineering Fracture Mechanics* **1**, 547–564. A cracked column under compression.
14. J. R. RICE and N. LEVY 1972 *Journal of Applied Mechanics* **39**, 185–194. The part-through surface crack in an elastic plate.
15. A. D. DIMAROGONAS 1970 *General Electric Co*, *Internal Report*. New York: Schenectady. Dynamic response of cracked rotors.
16. A. D. DIMAROGONAS 1976 *Vibration Engineering* St. Paul: West Publishers.
17. T. G. CHONDROS 1977 *M.Sc. Thesis*, *University of Patras*, *Greece*. Dynamic response of cracked beams.
18. T. G. CHONDROS and A. D. DIMAROGONAS 1979 *American Society of Mechanical Engineers Design Engineering Technical Conference*, *St. Louis*, *Paper* 79-*DET*-106. Identification of cracks in circular plates welded at the contour.
19. T. G. CHONDROS and A. D. DIMAROGONAS 1980 *Journal of Sound and Vibration* **69**, 531–538. Identification of cracks in welded joints of complex structures.
20. A. D. DIMAROGONAS and G. MASSOUROS 1980 *Engineering Fracture Mechanics* **15**, 439–444. Torsional vibration of a shaft with a circumferential crack.
21. R. D. ADAMS, P. CAWLEY, C. J. PYE and B. J. STONE 1978 *Journal of Mechanical Engineering Science* **20**(2), 93–100. A vibration technique for non-destructively assessing the integrity of structures.
22. P. CAWLEY and R. D. ADAMS 1979 *Journal of Strain Analysis* **14**, 49–57. The location of defects in structures from measurements of natural frequencies.
23. A. D. DIMAROGONAS and S. A. PAIPETIS 1983 *Analytical Methods in Rotor Dynamics*. London: Elsevier Applied Science.
24. N. ANIFANTIS and A. D. DIMAROGONAS 1983 *International Journal of Solids and Structures* **19**, 281–291. Stability of columns with a single crack subjected to follower and vertical loads.
25. P. GUDMUNDSON 1984 *Proceedings* 2*nd International Modal Analysis Conference*, V*olume* **2**, 690–697. Orlando, Union College, New York: Changes in modal parameters resulting from small cracks.
26. C. A. PAPADOPOULOS and A. D. DIMAROGONAS 1987 *Ingenieur Archiv* **57**, 257–266. Coupling of bending and torsional vibrations of a cracked Timoshenko shaft.
27. B. S. HAISTY and W. T. SPRINGER 1985 *Proceedings of the Society for Experimental Mechanics Spring Conference*, *Las Vegas*, 389–395. The longitudinal vibration characteristics of a uniform beam containing two symmetric discontinuities.
28. T. G. CHONDROS and A. D. DIMAROGONAS 1989 *Journal of Vibration*, *Acoustics*, *Stress and Reliability in Design* **111**, 251–256. Influence of cracks on the dynamic characteristics of structures.
29. A. D. S. BARR 1966 *Transactions of ASME Journal of Applied Mechanics* **33**, 465. An extension of the Hu-Washizu variational principle in linear elasticity for dynamic problems.
30. S. CHRISTIDES and A. D. S. BARR 1984 *International Journal Mechanics Science* **26**, 639–648. One-dimensional theory of cracked Bernoulli–Euler beams.

31. M. H. H. SHEN and C. PIERRE 1990 *Journal of Sound and Vibration* **138**, 115–134. Natural modes of Bernoulli–Euler beams with symmetric cracks.
32. M. H. H. SHEN and C. PIERRE 1990 *Journal of Sound and Vibration* **170**, 237–259. Free vibrations of beams with a single-edge crack.
33. A. D. DIMAROGONAS 1996 *Engineering Fracture Mechanics* **5**, 831–857. Vibration of cracked structures—a state of the art review.
34. H. C. HU 1955 *Scientia Sinica* **4**, 33–55. On some variational principles in the theory of elasticity and plasticity.
35. K. WASHIZU 1955 *Technical Report* 25–18, *Contract No. N*5–07833. Cambridge, MA: Massachussetts Institute of Technology. On the variational principles of elasticity and plasticity.
36. I. S. SOKOLNIKOFF 1956 *Mathematical Theory of Elasticity*. New York: McGraw-Hill; second edition.
37. R. CUNTZE and M. HAJEK 1985 *Ingenieur-Archiv* **55**, 237–241. Eigenfrequenzen eines angerissenen. Kragträgers Springer-Verlag.
38. J. WAUER 1990 *International Journal Solids and Structures* **26**, 901–914. Modeling and formulation of equation of motion for cracked rotating shafts.

APPENDIX: NOMENCLATURE

a	crack depth
A	beam cross-sectional area
c	local crack flexibility
c_0	material constant
E	Young's modulus of elasticity
$e = (\gamma_{xx} + \gamma_{yy} + \gamma_{zz})$	volume dilatation
$f(x)$	crack disturbance function
F_i	body forces
g_i	surface traction
G	Shear modulus of elasticity
G_n, H_n	constants
h	cross-section height
I	cross-sectional area moment of inertia
J_s	strain energy density function
K_I	stress intensity factor
L	length of beam
n_j	direction cosine
p_i	momentum
S_g, S_u	external surfaces
$S(x,t)$	strain function
$T(x,t)$	stress function
T_m	kinetic energy density
u_i	displacement field components
u_0	axial displacement of the uncracked beam
u^*	axial displacement due to crack
U_T	strain energy due to crack
V	total volume of the solid
$W(\gamma_{ij})$	strain energy density function
$w(x, t)$	lateral displacement function
w_0	lateral displacement of the uncracked beam
w^*	lateral displacement due to crack
α	crack ratio a/h
β	non-dimensional crack location
β_n^*	cracked beam natural frequency parameter
γ_{ij}	strain tensor components
δ_{ij}	Kronecker's delta
θ^*	additional rotation due to crack
λ	Lamé's constant
ν	Poisson ratio

ρ	material density
σ_{ij}	stress tensor components
υ	displacement at crack tip region
$\phi(x)$	mode disturbance function
ω_n	natural frequencies of the uncracked beam
ω_n^*	natural frequencies of the cracked beam
ω_{Ln}	natural frequencies of the cracked beam with lumped crack flexibility